How multipath error influences modernized GNSS ambiguity resolution in urban areas

Nobuaki KUBO, Akio YASUDA
Tokyo University of Marine Science and Technology (E-mail: nkubo@e.kaiyodai.ac.jp)

ABSTRACT

Commercial uses of GPS have been growing rapidly with applications for aircraft, ship, and land vehicle navigation as well as for surveying and time keeping. The next generation GPS and Japanese QZS (Quasi Zenith Satellite) will provide three different civil signals. Galileo will also provide several types of civil signals. The availability of the third civil frequency has obvious advantages to instantaneous carrier phase accuracy and ambiguity resolution for centimeter level measurements. This paper discusses the effects of additional new civil signals for the high accuracy positioning in urban areas based on simulation using practical raw data. As for constellation, only GPS and GPS+QZS are considered. For positioning, a short distance baseline is assumed in order to disregard atmosphere effects.

In this simulation, mask angle and signal conditions were fixed and ambiguity success rates were compared between different triple frequency combination scenarios. The coefficient of reflection was set randomly from 0.05 to 0.5 and the multipath delay was also set randomly from 5-100 m. Visible satellites and signal strength were determined by raw data collected in Tokyo by car. These simulation results have confirmed that the availability of high accuracy positioning will increase in all scenarios if we use GPS+QZS with triple frequencies.

Key words: multipath, ambiguity resolution, GNSS modernizatio

1. Introduction

The motivation behind this research was to answer the following question: "How many epochs within a day is it possible to resolve single epoch ambiguity resolution for centimeter level accuracy in urban areas?". Instantaneous ambiguity resolution has several advantages. It is resistant to negative effects of cycle slips and can provide centimeter-level positioning accuracy immediately, with no delay necessary for initialization for short distances. Since every epoch is virtually independent, loss of lock, a cycle slip, or a change in the tracked satellite constellation does not introduce additional complications to the data processing. The performance of this method is strongly dependent on the distance from the base station. Even in the case of short distances, it is difficult to resolve correct ambiguities in a single epoch due to the insufficient number of visible satellites and multipath errors in urban areas.

The modernization of GPS, the advent of QZS and the establishment of GALILEO will propel satellite-based positioning and navigation applications to such a level that the positioning reliability, integrity, availability, and accuracy will be improved tremendously. One significant benefit to high precision positioning brought by modernized GPS and GALILEO is that carrier phase integer ambiguity resolution will be greatly facilitated by involving triple carrier frequencies. During the past few years, a lot of research work has focused on algorithm studies for integer ambiguity resolution making use of three carrier frequencies [1,2]. Experimental tests using signal simulators and receivers for triple frequencies have been demonstrated by our group [3]. The main purpose of this paper is to study the achievable performance in the instantaneous ambiguity resolution in urban areas using a cascading ambiguity resolution method.

The outline of this paper is as follows: Section 2 shows the cascading ambiguity rounding algorithm including statistical testing in order to resolve correct ambiguities in a single epoch. Section 3 starts with a general discussion of the error sources in the measurement, especially multipath errors and discusses how to generate the raw pseudorange and carrier phase of triple frequencies. The simulation flow using real raw data is discussed in this section. The configuration of QZS is also discussed briefly in this section. Section 4 sets up a few simulated tests over short baselines and presents the corresponding test results together analysis. Section 5 summarizes this research and also discusses some ideas for further improvements.

2. Integer Ambiguity Resolution

2.1 Multi-Frequency Integer Ambiguity Resolution

The ambiguities can be determined using pseudo-range and carrier phase data directly. Unfortunately the accuracy of C/A or P-code pseudo-range is not good enough to determine the integer ambiguities because the wavelength of the carrier phase observable is only 19.03cm for L1, 24.42cm for L2 and 25.48cm for L5. It is very difficult, if not impossible, to determine integer ambiguity for one-way data because they suffer from clock divergence between the satellite and receiver. Therefore, the double-differenced carrier phase ambiguities should be formed and resolved to their integer values. The fundamental measurements from the GPS system will be three pseudo-range and three carrier phase measurements. The observation equations can be written as:

$$R_1 = \rho + \frac{I}{f_1^2} + \varepsilon_{R_1}, \quad R_2 = \rho + \frac{f_1^2}{f_2^2}\frac{I}{f_1^2} + \varepsilon_{R_2}, \quad R_3 = \rho + \frac{f_1^2}{f_3^2}\frac{I}{f_1^2} + \varepsilon_{R_3} \tag{1}$$

$$\varphi_1 = \rho - \frac{1}{\lambda_1}\frac{I}{f_1^2} + N_1 + \varepsilon_{\varphi_1}, \quad \varphi_2 = \rho - \frac{f_1^2}{f_2^2\lambda_1}\frac{I}{f_2^2} + N_2 + \varepsilon_{\varphi_2}, \tag{2}$$

$$\varphi_3 = \rho - \frac{f_1^2}{f_3^2\lambda_3}\frac{I}{f_1^2} + N_3 + \varepsilon_{\varphi_3}$$

The linear combination of carrier phase measurements for the triple-frequency case can be defined as:

$$\varphi_{i,j,k} = i\cdot\varphi_1 + j\cdot\varphi_2 + k\cdot\varphi_3 \tag{3}$$

and the observation equation can be derived as:

$$\varphi_{i,j,k} = \frac{\rho}{\lambda_{i,j,k}} - \frac{i + 77j/60 + 154k/115}{i + 60j/77 + 115k/154}\frac{1}{\lambda_{i,j,k}}\frac{1}{f_1^2} + N_{i,j,k} + \varepsilon_{\varphi_{i,j,k}} \tag{4}$$

The following effective frequency, wavelength and integer ambiguity combinations can be formed:

$$f_{i,j,k} = i \cdot f_1 + j \cdot f_2 + k \cdot f_3 \quad (5)$$

$$\lambda_{i,j,k} = c / f_{i,j,k} \quad (6)$$

$$N_{i,j,k} = i \cdot N_1 + j \cdot N_2 + k \cdot N_3 \quad (7)$$

If it is assumed that the standard deviations of random errors on the three frequencies are equal to M_0 [cycle], expressed in units of cycles of the corresponding wavelength, the standard deviation M [cycle] of the linear combination is:

$$M_{i,j,k}[cycle] = \sqrt{i^2 + j^2 + k^2} \cdot M_0[cycle] \quad (8)$$

$$M_{i,j,k}[m] = M_{i,j,k}[cycle] \cdot \lambda_{i,j,k} \quad (9)$$

These formulae clearly show that the random error, expressed in cycles of the effective wavelength, is always greater than the noise on either L1, L2 or L5 carrier phase measurements. However, the noise level for combinations in units of meters may be smaller than the noise on either L1, L2 or L5 carrier phase measurements. The ionosphere delay (in meters) on the range $\varphi_{i,j,k} \cdot \lambda_{i,j,k}$ can be represented as:

$$d^{ion}_{i,j,k} = K_{i,j,k} \cdot \frac{1}{f_1^2} \quad (10)$$

where $K_{i,j,k}$ is the ratio value between the ionospheric delays on the combinations (in units of meter) and the L1 carrier phase measurement, derived as follows:

$$K_{i,j,k} = \frac{i + 77j/60 + 154k/115}{i + 60j/77 + 115k/154} \quad (11)$$

There are many combinations without ionospheric delay effect. However, they could be derived from the three fundamental ionosphere-free combinations $\varphi_{77,-60,0}, \varphi_{154,0,-115}$ and $\varphi_{0,24,-23}$. This means that there are opportunities to find the optimal ionosphere-free combination for different purposes. For positioning purposes, the minimal variance for the ionosphere-free combination is desired, which means that the combinations have $K_{i,j,k} = 0$ and small $M_{i,j,k}[m]$. For ambiguity resolution purposes, the longest wavelength of the ionosphere-free combination is desired, which means that the combinations should have $K_{i,j,k} = 0$, $f_{i,j,k} = \min$ and small $M_{i,j,k}[m] = \min$. It can be proven from equation (5) that the minimum frequency among all combinations is 10.23 MHz. Although many different combinations with minimum frequency can be found, Table 1 shows some typical carrier phase combinations with long wavelength. $M_0[cycle]$ is assumed to be small multipath condition and is set 0.05/19.03 (= 5 mm) in the case of L1 signal.

Table 1. Typical Carrier Phase Combinations

$\varphi_{i,j,k}$	$f_{i,j,k}[MHz]$	$\lambda_{i,j,k}[m]$	$M_{i,j,k}[m]$	$K_{i,j,k}$
$\varphi_{-6,1,7}$	10.23	29.305	13.588	717.22
$\varphi_{-1,8,-7}$	10.23	29.305	15.645	-16.52
$\varphi_{3,0,-4}$	20.46	14.653	3.663	-180.45
$\varphi_{-3,1,3}$	30.69	9.7684	2.129	118.1
$\varphi_{1,-7,6}$	40.92	7.3263	3.397	1.98
$\varphi_{0,1,-1}$	51.15	5.861	0.414	-1.72
$\varphi_{1,-6,5}$	92.07	3.256	1.282	-0.07
$\varphi_{1,-1,0}$	347.82	0.862	0.061	-1.28
$\varphi_{1,0,-1}$	398.97	0.751	0.053	-1.34

So which combinations should be used for ambiguity resolution? Han and Rizos [4] concluded that $\varphi_{0,1,-1}$ is suitable for the starting point for ambiguity resolution. The signal by this combination is sometimes called extra-wide-lane signal. No matter how long the baseline is, $N_{0,1,-1}$ can be fixed using pseudo-range measurements directly, which means that the widelane carrier phase measurements of L2 and L5 are always available without ambiguity. They could be used for positioning with standard deviation of 40 cm (assuming $\sigma_\varphi = 5mm$) and ionospheric effect $-1.74 \cdot I / f_1^2$ in meters. It is important to note that the performance of this technique suffers from measurement noise and multipath effects. In this paper, this extra-wide-lane signal is used as a starting point for the triple frequency ambiguity resolution. In the case of using only two frequencies (L1 and L2), a wide-lane ($\varphi_{1,-1,0}$) signal for the ambiguity resolution is used.

2.2 Search and Validation Method

The flowchart of the ambiguity resolution used in this paper is shown in Fig. 1. The details are briefly described step by step as follows:

(1) The initial estimations of extra-wide-lane ambiguities are determined using the position, which is derived from the double differences of L1 pseudo-ranges. Non-smoothed pseudoranges are used because the target is the instantaneous precise positioning in this simulation. One sigma of the double differences of L1 pseudorange is set according to the linear combinations. This means that larger wavelength by linear combinations allows for large pseudorange errors. Performing an active search of the correct solution at each epoch is an adequate strategy for the resolution of the ambiguities. This search is carried out over a measurement or a positioning domain centered around an estimate of the solution. Numerous methods have been proposed so far and it has been investigated by Kim and Langley [5]. Our searching method is based on the method described by Hatch *et al* [6]. Among the observed satellites, four that have minimum PDOP are chosen as primary satellites. Ambiguities of primary satellites are resolved, the probable positions of the user receiver are obtained. First, the ambiguities of primary satellites are resolved by the least square searching method. Next, the ambiguities of the secondary satellites are resolved. Since the wavelength of extra-wide-lane is about 5.8m, the solution is within ± 1 cycles of the initial value with a confidence level of over 99%.

(2) Receiver position is assumed from ambiguity candidates. Statistical tests are performed in both the measurement domain and the positioning domain to identify the most probable position. In the measurement domain, the χ^2 test is applied using the sum of measurement residuals. The candidates satisfying the fixed condition are rejected. In the positioning domain, taking the differences between the horizontal positions deduced by the pseudo-range and the ambiguity candidate, the candidates that fit into the criteria are selected. The confidence level is set at 99% in both statistical tests. In order to select the one candidate in a single epoch, the candidate with minimum residual is chosen.

(3) The initial values of wide-lane ambiguity are deduced from the position determined by the extra-wide-lane technique.

(4) The procedures of wide-lane ambiguity resolution are almost

same as the extra-wide-lane ambiguity resolution, but the search range has to be enlarged.

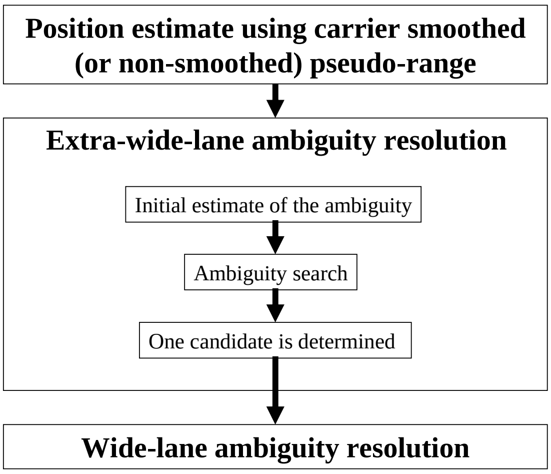

Figure 1. Flowchart of RTK algorithm

3. The GNSS simulator

3.1 Outline of the GNSS simulator

A software simulator to analyse the precise positioning performance under urban conditions has been developed. In order to simulate the positioning performance, it needs the satellites orbits, signal structure, the receiver's parameters and its position. The simulator can generate DLL and PLL tracking errors, which are defined respectively as the difference between the true code pseudo-range or carrier phase and the measured one. These are obtained by equations (12) and (13) which model the errors in DLL and PLL tracking loops of the receiver. These equations are written in Kaplan [7]. It can also generate multipath errors by adding some parameters. The clock error is neglected because of the usage of double differenced data in the positioning. The propagation and satellite errors are also neglected because of short baseline assumption.

In order to simulate the urban condition performance, raw GPS data collected in Tokyo be car are used. In 2005, the data was repeatedly collected in downtown Tokyo using the NovAtel OEM4 receiver. 12 hours of raw GPS data are generated by combining several data periods. The rover satellite configuration and the carrier to noise ratio on each satellite are based on the raw GPS data. On the other hand, the reference carrier to noise ratio on each satellite is calculated as a function of the elevation.

$$\sigma_t DLL = \lambda_c \sqrt{\frac{4F_1 d^2 B_w}{c/n_0}\left[2(1-d)+\frac{4F_2 d}{Tc/n_0}\right]}\ (m) \quad (12)$$

$$\sigma_t PLL = \frac{\lambda_L}{2\pi}\sqrt{\frac{B_w}{c/n_0}\left[1+\frac{1}{2Tc/n_0}\right]}\ (m) \quad (13)$$

where λ_c is code chipping rate (293.05m for C/A code). F_1 is DLL discriminator correlator factor (=1/2). F_2 is DLL discriminator type factor (=1). d is correlator spacing between early and late. B_w is code or carrier loop noise bandwidth (Hz). c/n_0 is carrier to noise power ratio ($C/N_0 = 10^{c/n_0/10}$).T is predetection integration time (sec). λ_L is wavelength for L-band signal (0.1903m for C/A code). A wide-band (20MHz) GPS receiver tracking C/A code type signal on L1, L2 and L5 separately is simulated. The receiver parameters are shown in Table 2. The flowchart of the precise positioning used in this paper is shown in Fig. 2.

Table 2. Receiver Parameters

DLL loop bandwidth	0.05 Hz
PLL loop bandwidth	5 Hz
DLL detector	Early-late power
PLL detector	Sinus
Correlator spacing	0.1 (strobe in L1,L2)

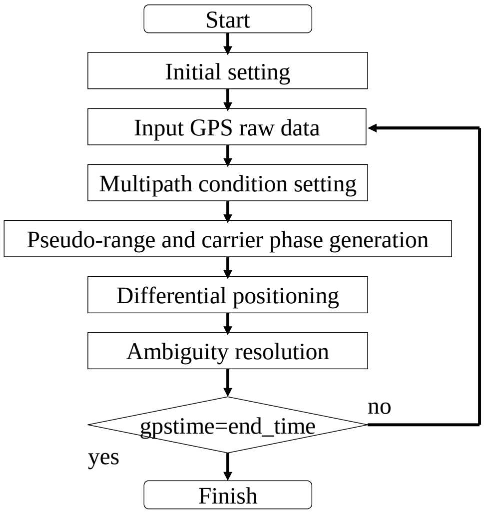

Figure 2. Flowchart of precise positioning

3.2 Generation of the multipath errors

Multipath refers to the phenomenon of a signal reaching an antenna via two or more paths. Typically, an antenna receives the direct (line-of-sight) signal and one or more of its reflections from the structures in the vicinity and from the ground. A reflected signal is a delayed and usually weaker version of the direct signal. The range measurement error due to multipath depends on the strength of the reflected signal and the delay between the direct and reflected signals. Multipath affects both code and carrier measurements, but the magnitudes of the error differ significantly. The effect of multipath can be reduced in antenna design and also in the signal processing step in a receiver.

Since it was impossible to extract the multipath errors from the raw GPS data in the car, multipath errors were set artificially as follows in order to reflect the urban multipath effects in this simulation.

(1) Multipath errors from the ground were set throughout the simulation period in the reference and rover station depending on the antenna height and the electric properties of the ground.
(2) Multipath errors from the structures were set in the rover station throughout the simulation period. One or two satellites were randomly selected for setting multipath. Multipath amplitudes were set according to the elevation from 0.05 to 0.5. Multipath delays were set randomly from 5m to 100m.
(3) When the pseudorange or carrier phase was generated, the above multipath errors were added to them.

3.3 Constellation of the satellites

The GPS constellation is determined by the raw GPS data described in the section 3.1. Since QZS constellation parameters have not been decided yet, one constellation case was chosen for the simulation. The satellite inclination is 45°. It will improve satellite communication environment for mobile users in urban and mountainous areas by offering elevation angles of higher than about 70° at all time over a Japanese islands. If the satellite orbits are appropriately selected, one satellite stays over Japan and the surrounding area with a high elevation angle for at least 8 hours. Therefore, three satellites are sufficient with three inclined orbits having the longitude of ascending node of 120° separation for 24-hour operation. The constellation shown in Fig. 3 is with three elliptical orbital planes having one satellite. Key-parameters are an eccentricity of 0.099, a perigee height of 31612 km, an apogee height of 39960 km and an inclination of 45°. L1, L2 and L5 signals are used in both GPS and QZS in this simulation. Signal parameters are shown in Table 3.

Table 3. Signal Parameters, GPS and QZS space segment

Frequency band:	L1	L2	L5
Carrier frequency [MHz]	1575.42	1227.6	1176.45
Code rate [MHz]	1.023	1.023	10.23
Bandwidth[MHz]	20	20	20
Received signal power [dBm]	-158	-165	-158

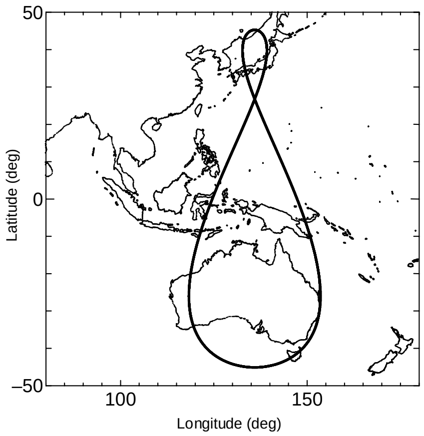

Figure 3. QZS constellation

4. The performance of GPS-QZS triple frequency precise positioning

4.1 Scenarios of the simulation

In order to evaluate the performance of the precise positioning, the ambiguity fix percentages using the above simulator were calculated: GPS with L1 and L2 signals, GPS with L1, L2 and L5 signals, GPS combined QZS with L1, L2 and L5 signals. Each scenario has been tested under two types of correlators: narrow correlator and strobe correlator. The model parameters and basic assumptions are briefly reviewed as follows. Only short baseline within 1 km is considered. Differential atmospheric delays are assumed to be completely absent (zero) between reference and rover receivers. In order to simulate the urban condition performance, the raw GPS data were used. The data was repeatedly collected in downtown Tokyo using the NovAtel OEM4 receiver. 12 hours of raw GPS data are generated by combining several data periods. Satellite elevation cut-off angle is 10 degrees.

The ambiguity fix percentage is adopted here as an indicator of the performance. The ambiguity is computed for all 43,200 epochs (12 hours). The integer ambiguity is re-initialized every second. The ambiguity fix percentage can be obtained by calculating the ratio value between the number of correct ambiguity fixes and the number of the total ambiguity fixes. Single epoch ambiguity resolution procedure requires 5 or more satellites.

4.2 Relative frequency distribution and DGPS results

Fig. 4 shows relative frequency distributions versus the number of visible satellites in both cases of GPS and GPS+QZS constellations. There are 5 or more visible satellites in downtown Tokyo for approximately 63% of the 12 hours data collection period in the current GPS constellation. Therefore, the service of precise positioning is not practical, as the single epoch ambiguity resolution procedure requires a minimum of 5 satellites. On the contrary, 5 or more satellites are available over 84% of 12 hours period in the combined GPS and QZS constellation. Adding three QZS improved availability around 21% in terms of RTK service. Table 4 shows the distribution of the absolute DGPS horizontal errors in the current GPS constellation. Table 5 shows the distribution of the absolute DGPS horizontal errors in the combined GPS and QZS constellation. The second line shows the results of using a strobe correlator (0.1chip). The third line shows the results of using a narrow correlator (0.1chip).

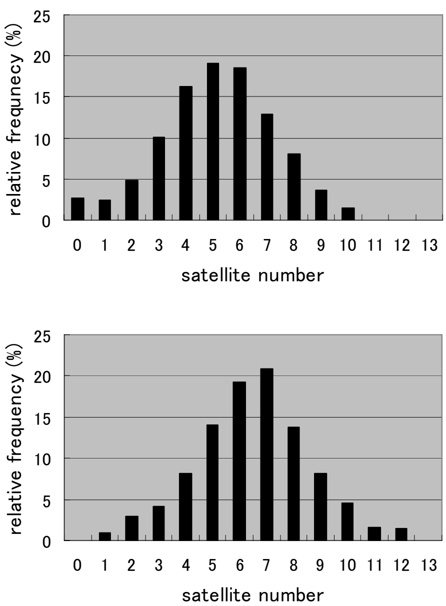

Figure 4. Relative frequency distribution (GPS and GPS+QZS)

With a minimum of 4 visible satellites, the position can be calculated. Adding three QZS improved availability of DGPS (from 79.5% to 91.9%), however, the accuracy is not significantly different. This is because most of the errors in DGPS is due to multipath errors. It is clear that the strobe correlator can reduce multipath errors compared to the narrow correlator. This is because the strobe correlator does not suffer from the influence of multipath which is over 30-40m delayed from the direct path. The usual horizontal errors in DGPS in open sky are less than 1.0m over 99%.

Table 4. Distribution of the absolute DGPS horizontal errors (GPS: 34356epoch)

Horizontal Errors(m)	0-1	1-2	2-4	4-6	6-10	10-
Strobe(%)	73.8	16.0	6.5	1.3	1.1	1.3
Narrow(%)	33.5	26.7	26.6	6.6	3.5	3.1

Table 5. Distribution of the absolute DGPS horizontal errors (GPS+QZS: 39704epoch)

Horizontal Errors(m)	0-1	1-2	2-4	4-6	6-10	10-
Strobe(%)	72.2	17.8	6.2	1.4	1.1	1.3
Narrow(%)	39.0	27.0	24.5	4.8	2.6	2.1

4.3 GPS with dual frequencies (L1 and L2)

Table 6 shows the ambiguity fix percentage for GPS with dual frequencies for the two types of correlators. The second column gives the percentage of single epoch ambiguity resolution fixes, while the third column gives the wrong ambiguity fix percentage. The fourth column gives the percentage of times in which the number of satellites is less than 5. At least 5 satellites are needed in the ambiguity resolution.

In the case of strobe correlator, the single epoch ambiguity fix percentage is about 40 %. Comparing the two correlators, it is found that the strobe correlator plays an important role in increasing the ambiguity fix percentage. This means that the narrow correlator receiver is badly influenced by the medium delay multipath (from 30m to 100m).

Table 6. Ambiguity Fix Percentage (GPS with L1 and L2 signals)

	1epoch Fix (%)	Wrong (%)	No-RTK (%)
Strobe correlator	40.0	22.8	37.2
Narrow correlator	24.5	38.4	37.2

4.4 GPS with triple frequencies (L1,L2 and L5)

Table 7 shows the ambiguity fix percentage for GPS with triple frequencies for the two types of correlators. There are two types of results in the table. One is the result for extra-wide-lane(left side), and the other result for wide-lane(right side). Linear combination of L2 and L5 is used in the extra-wide-lane. Linear combination of L1 and L2 is used in the wide-lane. The initial values of wide-lane ambiguities are deduced from the position determined by extra-wide-lane technique.

In the case of strobe correlator, the single epoch ambiguity fix percentage is about 61% for extra-wide-lane and 58% for wide-lane. This is mainly due to lack of visible satellites. The single epoch ambiguity fix percentage during periods with over 5 visible satellites is relatively high (60.5/62.8=96.3% for extra-wide-lane, 58.3/62.8=92.8% for wide-lane). Comparing the results of dual frequency, the single epoch ambiguity fix percentage is considerably improved even in the case of wide-lane. This is because the initial values of wide-lane ambiguities from extra-wide-lane are more accurate than the initial values of wide-lane ambiguities from DGPS. Comparing the two correlators, it is also found that the strobe correlator plays an important role in increasing the ambiguity fix percentage.

Table 7. Ambiguity Fix Percentage (GPS with L1, L2 and L5 signals)

	1epoch Fix (%)	Wrong (%)	No-RTK (%)
Strobe correlator	60.5/58.3	2.3/4.5	37.2
Narrow correlator	51.6/49.9	11.2/12.9	37.2

4.5 Combined GPS and QZS with triple frequencies (L1, L2 and L5)

Table 8 shows the ambiguity fix percentage for combined GPS and QZS with triple frequencies for the two types of correlators. There are also two types of results in the table.

Adding three QZS improved availability of periods with over 5 visible satellites from 62.8% to 83.6%. This is clearly a good influence the ambiguity resolution. In the case of the strobe correlator, the single epoch ambiguity fix percentage is about 81% for extra-wide-lane and 80% for wide-lane. This is also mainly due to lack of visible satellites. The single epoch ambiguity fix percentage during periods with 5 or more visible satellites is relatively high (80.7/83.6=96.5% for extra-wide-lane, 79.8/83.6=95.5% for wide-lane) and similar to the cases of GPS with triple frequencies. Comparing the two correlators, it is also found that the strobe correlator plays an important role in increasing the ambiguity fix percentage. The increase of the available period for ambiguity resolution is directly proportional to the increase of the single epoch ambiguity fix percentage. It means that the increase of visible satellites is a key to ambiguity resolution if the receiver can receive triple frequencies with the latest multipath mitigation correlator.

Table 8. Ambiguity Fix Percentage (GPS and QZS with L1, L2 and L5 signals)

	1epoch Fix (%)	Wrong (%)	No-RTK (%)
Strobe correlator	80.7/79.8	2.9/3.8	16.4
Narrow correlator	71.6/71.0	12.0/12.6	16.4

5. Summary and Conclusions

The GNSS simulator was developed to simulate the performance of single epoch ambiguity resolution in urban areas. In order to simulate more realistically, raw GPS data collected in Tokyo be car were used. Using this GNSS simulator, it was demonstrated that centimeter-level instantaneous RTK GPS in urban areas was feasible when the receiver can use modernized triple frequencies with the latest multipath mitigation correlator. Also, the increase of visible satellites was a key to ambiguity resolution in urban areas because the single epoch ambiguity resolution procedure requires 5 or more satellites. From this point of view, Japanese QZS will provide not only good availability but also good ambiguity fix rates in Japan. In this simulation, the strobe correlator with 20MHz bandwidth was used as the latest multipath mitigation technique. This type of correlator can significantly reduce multipath errors of over 30-40m multipath delay. Fortunately, owing to the advent of L5 frequency, a special correlator does not have to be used because the multipath mitigation performance of standard correlator of L5 frequency is similar to the performance of strobe correlator of L1 frequency. In urban areas, multipath delay within 100m is dominant and the further improvement will be expected in order to reduce short delay multipath of within 30-40m.

References

1. Hatch R. (1996): The promise of a third frequency, GPS WORLD, May 1996, 55-58

2. Teunissen, P., Joosten, P. and Tiberius, C. (2002): A Comparison of TCAR, CIR and LAMBDA GNSS Ambiguity Resolution, ION GPS 2002, pp. 2799-2808.

3. Kubo, N.,Yasuda, A.,Kawano, I.,Ono, T. and Uratani, C. (2006): The Benefits of Three Frequencies for the High Accuracy Positioning, ENC2006

4. HAN, S., & RIZOS, C., (1999): The impact of two additional civilian GPS frequencies on ambiguity resolution strategies, 55th National Meeting U.S. Institute of Navigation, "Navigational Technology for the 21st Century", Cambridge, Massachusetts, 28-30 June, pp. 315-321.

5. Kim, D. and Langley, R.B., (2000): GPS Ambiguity Resolution and Validation: Methodologies, Trends and Issues, 7th GNSS workshop, Seoul,Korea,November.

6. Hatch R. (1991): Instantaneous Ambiguity Resolution , Proceedings of International Association of Geodecy Symposia 107 on KinematicSystems in Geodecy, Surveying and Remote Sensing, New York, Springer-Verlag, pp. 298-308

7. Kaplan, E. D. (1996): Understanding GPS Principles and Applications, Artech House Publishers, Boston, London, pp. 157-172.